



**HAL**  
open science

## Quaternionic wavelets for texture classification

Raphaël Soulard, Philippe Carré

► **To cite this version:**

Raphaël Soulard, Philippe Carré. Quaternionic wavelets for texture classification. *Pattern Recognition Letters*, 2011, 32 (13), pp.1669–1678. <10.1016/j.patrec.2011.06.028>. <hal-00618159>

**HAL Id: hal-00618159**

**<https://hal.science/hal-00618159v1>**

Submitted on 31 Aug 2011

**HAL** is a multi-disciplinary open access archive for the deposit and dissemination of scientific research documents, whether they are published or not. The documents may come from teaching and research institutions in France or abroad, or from public or private research centers.

L'archive ouverte pluridisciplinaire **HAL**, est destinée au dépôt et à la diffusion de documents scientifiques de niveau recherche, publiés ou non, émanant des établissements d'enseignement et de recherche français ou étrangers, des laboratoires publics ou privés.



HAL Authorization

# Quaternionic Wavelets for Texture Classification

Raphaël Soulard, Philippe Carré

*XLIM-SIC laboratory - CNRS UMR 6172 - University of Poitiers, France*

---

## Abstract

This article proposes a study of the recent quaternionic wavelet transform (QWT) from a practical point of view through a digital image analysis application. Based on a theoretic 2D generalization of the analytic signal leading to a strong 2D signal modeling, this representation uses actual 2D analytic wavelets and yields subbands having a shift-invariant magnitude and a 3-angle phase, using the quaternion algebra.

Our experiment furthers the understanding of this quite sophisticated tool, and shows its practical interest by a clear improvement of a famous wavelet application : texture classification. Thanks to coherent multiscale analysis brought by the QWT we obtain better classification results than with standard wavelets in a similar process.

*Keywords:* Wavelet transform, 2D Phase, Quaternionic Wavelet Transform, Image texture analysis, Image classification

---

*Email addresses:* [raphael.soulard@univ-poitiers.fr](mailto:raphael.soulard@univ-poitiers.fr) (Raphaël Soulard),  
[carre@sic.univ-poitiers.fr](mailto:carre@sic.univ-poitiers.fr) (Philippe Carré)

## 1. Introduction

Since the 90's wavelets have been widely used for the analysis of textural images [Tuceyran and Jain, 1993; Lasmar and Berthoumieu, 2010]. Accordingly the human visual system sees textures through different channels related to particular frequency bands and directions; and wavelet representations offer this kind of decomposition. So by extracting simple features from each subband, the image content can be characterized separately at different scales and orientations, making an efficient texture analysis.

In 2001, the well known power of the *analytic signal* for signal modeling led to a new definition of wavelets : the *Complex Wavelet Transform* (CWT) [Selesnick et al., 2005], whose subbands are *analytic signals* giving access to a shift-invariant amplitude envelope (*magnitude*). The CWT codes signals in a more coherent way than standard wavelets (DWT); which overcomes their famous shift-variance problem. Its superiority over DWT for texture analysis has been shown in [de Rivaz and Kingsbury, 1999; Celik and Tjahjadi, 2009]. But CWT *phase* is ambiguous for 2D signals and is almost not used in applications excepted in a very recent work [Celik and Tjahjadi, 2011]. In parallel, the work in [Bülow, 1999] provides a strong theoretic 2D generalization of the *analytic signal* defined in quaternion algebra. The 3-angle *local 2D phase* related to it contains 2D geometric information. The *Quaternionic Wavelet Transform* (QWT) - first proposed in 2004 [Chan et al., 2008; Bayro-Corrochano, 2006] - uses wavelets that are 2D-analytic in the sense of Bülow, providing quaternion valued subbands with shift-invariant *magnitude* and this new 2D *phase*. This representation - specially defined for 2D signals - is a great theoretic improvement of CWT yielding a coherent description

26 of local 2D structures.

27 Currently, many evolutions of wavelets focus on *directionality* (Contour-  
28 lets, Complex Wavelets, Directionlets, Adaptive lifting schemes); bringing  
29 some redundancy to fit numerous directions from a quite algorithmic point  
30 of view. QWT is a different approach to a coherent representation of local  
31 structures in images based on a strong 2D signal processing theory; and sets  
32 some redundancy in a *local phase* rather than in directionality.

33 Given the promising theoretical properties of this new transform, we pro-  
34 pose here a global study of this sophisticated tool to further its understanding  
35 through a famous application of wavelets. We aim to show its potential and  
36 verify its practical superiority over standard DWT in a comparative texture  
37 analysis application.

38 The main point is the understanding of the information carried by QWT  
39 coefficients. QWT magnitude can intuitively be used like DWT but interpre-  
40 tation of phase is far from straightforward. With a first QWT based feature  
41 extraction algorithm this work gives an application not did yet to our knowl-  
42 edge and furthers practical use of QWT coefficients. We expect QWT to  
43 provide better texture analysis than DWT - with simple feature extraction  
44 methods - thanks to better separation of information and shift-invariance.  
45 An additional experimental comparison is done with CWT because the topic  
46 is near.

47 After a presentation of the transform, we propose several feature extrac-  
48 tion methods based on both DWT and QWT. To compare with literature,  
49 we also describe some CWT based feature descriptors recently published in  
50 [Celik and Tjahjadi, 2009, 2011]. The use of QWT phase is then discussed as

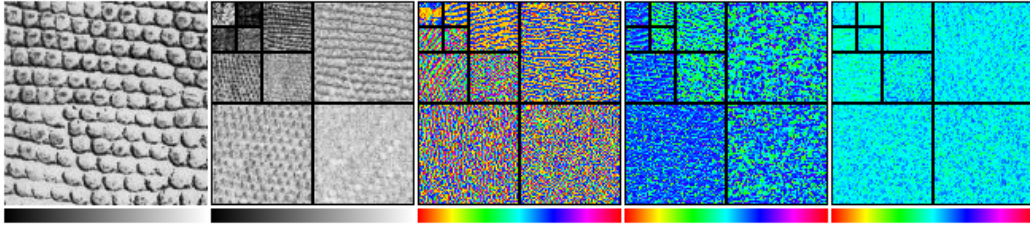


Figure 1: Quaternionic wavelet transform of a textural image. From left to right : Original image, magnitude  $|q|$  (intensity inverted for visual convenience),  $\varphi \in [-\pi; \pi]$ ,  $\theta \in [-\frac{\pi}{2}; \frac{\pi}{2}]$ ,  $\psi \in [-\frac{\pi}{4}; \frac{\pi}{4}]$ . The 3 terms of phase are represented in color - the hue corresponding to the angle (cyan for 0, red for  $\pm\pi$ ). Darker zones in phase correspond to negligible magnitude (making phase absurd).

51 well as the combination of QWT magnitude and phase based features. We  
 52 finally give experimental classification results to compare DWT and QWT in  
 53 terms of recognition rates. Note that the point is to observe changes in recog-  
 54 nition and not to get a competitive texture recognition performance. The  
 55 aim is to carry out a simple process to help us studying wavelet transforms,  
 56 rather than achieving excellent recognition. Types of texture better described  
 57 by one or another transform will be analyzed in terms of visual/geometric  
 58 content.

## 59 2. Quaternionic Wavelet Transform

60 The Quaternionic Wavelet Transform (QWT) is a perfect reconstruction  
 61 2D filterbank decomposition for grayscale images; addressing three common  
 62 drawbacks of standard DWT :

- 63 • Oscillations - Using oscillating wavelets complicates the representation  
 64 of a *simple* structure, involving several coefficients in a neighborhood

65 to compensate each other their own oscillations, and so making local  
66 analysis difficult.

- 67 • Shift-variance - The look of a wavelet transform may substantially  
68 change by a small shift of the image; causing incoherence while most  
69 recognition processes need invariant features.
- 70 • No phase notion - Fourier phase and local phase from the analytic  
71 signal are powerful analysis tools so it is interesting to fit DWT up  
72 with a phase notion in a pattern recognition context.

73 The key is to embed the *analytic signal* modeling into the wavelet frame-  
74 work. The *Dual-Tree* CWT [Selesnick et al., 2005] achieves 1D analytic  
75 wavelet analysis with a 2 times redundant perfect reconstruction filterbank  
76 overcoming the 3 drawbacks listed above. But its 2D version yields an am-  
77 biguous phase failing to efficiently describe local structures. More precisely,  
78 the phase angle encodes a local shift around pixel position - in the exact di-  
79 rection that is orthogonal to the intrinsic orientation of considered subband.  
80 Since the structure may be not well aligned with wavelet orientation, this  
81 shift information is not sufficient to accurately localize the structure.

82 The point then is the 2D generalization of analytic signal and the geo-  
83 metric meaning of the 2D phase extracted from it.

84 This is why the QWT uses the 2D analytic signal defined in [Bülow, 1999]  
85 within the quaternion algebra. According to Bülow, this generalization is  
86 superior to previous attempts in  $\mathbb{C}$  - including the one implicitly related to  
87 2D CWT - and is well adapted for 2D signals whereas standard complex  
88 analytic signal is only adapted in 1D. The extracted quaternionic local phase

89 (3 angles) contains rich geometric information. Note that Bülow proposed  
90 quaternionic Gabor filters in 1999 [Bülow, 1999] and used the phase for image  
91 analysis applications.

92 The QWT provides a quaternionic multiresolution analysis with 2D ana-  
93 lytic wavelets overcoming the above-cited drawbacks of DWT. Whereas DWT  
94 coefficients are real, QWT is quaternion valued *i.e.* 4-vectors made of one  
95 magnitude and a 3-angle phase. Information is better separated to describe  
96 more explicitly the image content. In 2004, the Rice University from Houston  
97 proposes to use their *Dual-Tree* algorithm to carry out a QWT with perfect  
98 reconstruction filterbanks [Chan et al., 2008] (that we use in this work). Note  
99 that at the same time, Bayro proposes a quaternionic Gabor pyramid [Bayro-  
100 Corrochano, 2006], windowing the *quaternionic Fourier transform* (QFT),  
101 but this approach has no perfect reconstruction so the use can be limited for  
102 example in image coding.

103 In this section we present the quaternionic 2D analytic signal upon which  
104 the QWT is based, the definition of the transform, the algorithm we used  
105 and the use of this tool.

### 106 2.1. The Quaternionic Analytic Signal

107 In his thesis [Bülow, 1999], T. Bülow showed that *complex* algebra  $\mathbb{C}$  is  
108 only adapted for handling 1D signals and that 2D signals are best described  
109 by embedding signal processing tools in the more general *quaternion* algebra  
110  $\mathbb{H}$ . He defined a ‘Quaternionic 2D Fourier Transform’ (QFT) and a ‘Quater-  
111 nionic 2D Analytic Signal’.

A quaternion is a generalization of a complex number, related to 3 imag-  
inary units  $i, j, k$  following the rules  $i^2 = j^2 = k^2 = -1$  and  $ij = -ji = k$ ; and

written  $q = a + bi + cj + dk$ . A polar form  $q = |q|e^{i\varphi}e^{j\theta}e^{k\psi}$  analogous to the complex one is defined by one modulus  $|q|$  and three angles  $(\varphi, \theta, \psi)$  called *phase*. The phase corresponds here to Euler angles in a 4D Euclidean space :

$$\begin{aligned}\varphi &= \operatorname{atan}(2(cd+ab), a^2-b^2+c^2-d^2)/2 + k\pi && \in [-\pi; \pi] \\ \theta &= \operatorname{atan}(2(bd+ac), a^2+b^2-c^2-d^2)/2 && \in [-\frac{\pi}{2}; \frac{\pi}{2}] \\ \psi &= \operatorname{arcsin}(2(ad-bc)/2) && \in [-\frac{\pi}{4}; \frac{\pi}{4}]\end{aligned}$$

112 with  $|q| = 1$ . See [Bülow, 1999] pp 16-21 for a detailed definition.

As a fundamental signal processing tool the *analytic signal* associated to a real 1D signal  $f(t)$  is well known to be constructed by setting its Hilbert transform  $\mathcal{H}f(t)$  in the imaginary part; being equivalent to a simple spectral operation :

$$f_A(t) = f(t) + i\mathcal{H}f(t) \Leftrightarrow \hat{f}_A(\omega) = \begin{cases} 0 & \text{if } \omega < 0 \\ \hat{f}(\omega) & \text{if } \omega = 0 \\ 2\hat{f}(\omega) & \text{if } \omega > 0 \end{cases}$$

113 Note that the spectrum of  $f_A$  is null for negative frequencies.

114 Modulus and argument of  $f_A$  can be interpreted as instantaneous *magni-*  
115 *tude* and *phase*. When the original signal is considered *oscillating* or narrow-  
116 band these two pieces of data become meaningful - making this tool useful  
117 for instance in amplitude and frequency modulation.

118 Looking at one point of interest, we can interpret a high magnitude as a  
119 strong ‘presence of some oscillation’ around this point. Phase indicates the  
120 relative location of this point within the oscillation.

121 Bülow pointed out that instantaneous phase equivalently describes the  
122 *kind* of structure at a point - among four fundamental structures : 0-‘positive

123 impulse',  $\pi/2$ -‘falling step’,  $\pm\pi$ -‘negative impulse’,  $-\pi/2$ -‘rising step’. This  
 124 is an important point for pattern recognition and that is why the author  
 125 wanted to generalize it for 2D signals.

126 Several generalizations to 2D are possible and depend on properties we  
 127 choose to keep. We consider 2D versions of the Hilbert transform (HT). The  
 128 partial HT ( $\mathcal{H}_\theta$ ) is equivalent to a 1D HT along direction  $\theta$ . The total HT  
 129 ( $\mathcal{H}_T = \mathcal{H}_0\mathcal{H}_{\pi/2}$ ) is the combination of two partial HT’s along  $x$  and  $y$  axes.  
 130 A 2D analytic signal of  $f$  can be constructed by adding  $\mathcal{H}_\theta f$  as the imaginary  
 131 part; what would cancel out a  $\theta$ -oriented half-plane in the frequency domain.  
 132 But this method depends on an arbitrary choice of the direction - not really  
 133 adapted for our issue. We can use as well  $\mathcal{H}_T$ ; what cancels out 3 quadrants  
 134 of the Fourier domain, but the original signal cannot be retrieved from the  
 135 analytic signal (This is the classical approach in [Hahn, 1996]).

So Bülow proposed to embed both partial and total HT’s into a quaternionic analytic signal :

$$f_A(x, y) = f(x, y) + i\mathcal{H}_0f(x, y) + j\mathcal{H}_{\pi/2}f(x, y) + k\mathcal{H}_Tf(x, y)$$

136 This method cancels out 3 quadrants of the (quaternionic) Fourier domain  
 137 and allows retrieval of the original signal. Its polar representation provides  
 138 2D local magnitude and phase that can be used to analyze 2D signals - in a  
 139 similar way as with 1D analytic signal.

140 The QWT uses this generalization to carry out an ‘actual’ 2D analytic  
 141 wavelet transform.

142 *2.2. Quaternionic Wavelets : Definition*

143 A standard wavelet transform (DWT) provides a scale-space analysis of  
 144 an image; yielding a matrix in which each coefficient is related to a ‘subband’  
 145 (localization in the 2D Fourier domain) and to a position in the image. A  
 146 ‘subband’ means both an oscillation scale (i.e. a 1D frequency band) and a  
 147 spatial orientation (i.e. rather vertical, horizontal or diagonal).

148 For 2D signals, the QWT provides a richer scale-space analysis than  
 149 DWT. Its coefficients are analytic according to Bülow’s theory and con-  
 150 trary to DWT the magnitude is near shift-invariant. Thus it inherits the  
 151 magnitude-phase local analysis from the very useful 1D analytic signal. In  
 152 the one hand the QWT can be viewed like a local ‘2D Quaternionic Fourier  
 153 Transform’ (QFT); in the other hand its subbands are ‘2D Quaternionic  
 154 Analytic Signals’ associated with bandpass filtered versions of the original  
 155 signal.

156 Note that usual interpretation of magnitude remains analogous to 1D as  
 157 it indicates the relative ‘presence’ of a local geometric *element*; whereas the  
 158 local phase is now represented by 3 angles carrying a complete description of  
 159 this 2D structure.

We start with real separable scaling function  $\phi$  and mother wavelets  $\psi^D$ ,  
 $\psi^V$ ,  $\psi^H$ , and we construct their analytic extensions in  $\mathbb{H}$  :

Real function :	Analytic extension :
$\psi^D = \psi_h(x)\psi_h(y)$	$\rightarrow \psi^D + i\mathcal{H}_0\psi^D + j\mathcal{H}_{\pi/2}\psi^D + k\mathcal{H}_T\psi^D$
$\psi^V = \phi_h(x)\psi_h(y)$	$\rightarrow \psi^V + i\mathcal{H}_0\psi^V + j\mathcal{H}_{\pi/2}\psi^V + k\mathcal{H}_T\psi^V$
$\psi^H = \psi_h(x)\phi_h(y)$	$\rightarrow \psi^H + i\mathcal{H}_0\psi^H + j\mathcal{H}_{\pi/2}\psi^H + k\mathcal{H}_T\psi^H$
$\phi = \phi_h(x)\phi_h(y)$	$\rightarrow \phi + i\mathcal{H}_0\phi + j\mathcal{H}_{\pi/2}\phi + k\mathcal{H}_T\phi$

Mathematically, 2D HT's of separable functions are equivalent to 1D HT's along rows and/or columns. So we consider the 1D Hilbert pair of wavelets and scaling functions :

$$(\psi_h, \psi_g = \mathcal{H}\psi_h) \quad (\phi_h, \phi_g = \mathcal{H}\phi_h)$$

and we have for instance :  $\mathcal{H}_0\psi^V = \mathcal{H}\phi_h(x)\psi_h(y) = \phi_g(x)\psi_h(y)$ . The analytic 2D wavelets can then be written in terms of separable products :

$$\begin{aligned} \psi^D &= \psi_h(x)\psi_h(y) + i\psi_g(x)\psi_h(y) + j\psi_h(x)\psi_g(y) + k\psi_g(x)\psi_g(y) \\ \psi^V &= \phi_h(x)\psi_h(y) + i\phi_g(x)\psi_h(y) + j\phi_h(x)\psi_g(y) + k\phi_g(x)\psi_g(y) \\ \psi^H &= \psi_h(x)\phi_h(y) + i\psi_g(x)\phi_h(y) + j\psi_h(x)\phi_g(y) + k\psi_g(x)\phi_g(y) \\ \phi &= \phi_h(x)\phi_h(y) + i\phi_g(x)\phi_h(y) + j\phi_h(x)\phi_g(y) + k\phi_g(x)\phi_g(y) \end{aligned}$$

160 From a practical point of view, the mother wavelet is related to a quaternionic  
 161 2D analytic filter - computable with separable 2D filterbanks. This means  
 162 the decomposition is heavily dependent on the position of the image with  
 163 respect to  $x$  and  $y$  axes (rotation-variance) and the wavelet is not isotropic  
 164 but the advantage is the easy computation.

165 Each subband from QWT can be seen as the analytic signal associated  
 166 with a narrowband part of the image. Shift-invariant magnitude  $|q|$  repre-  
 167 sents elements at any space position in each frequency subband; and phase  
 168  $(\varphi, \theta, \psi)$  describes the 'structure' of these elements. We discuss below the  
 169 interpretation of the phase.

### 170 2.3. Dual-Tree Implementation

171 The QWT is implemented by the Dual-Tree algorithm [Selesnick et al.,  
 172 2005] - a filterbank using a Hilbert pair as a complex 1D wavelet - originally

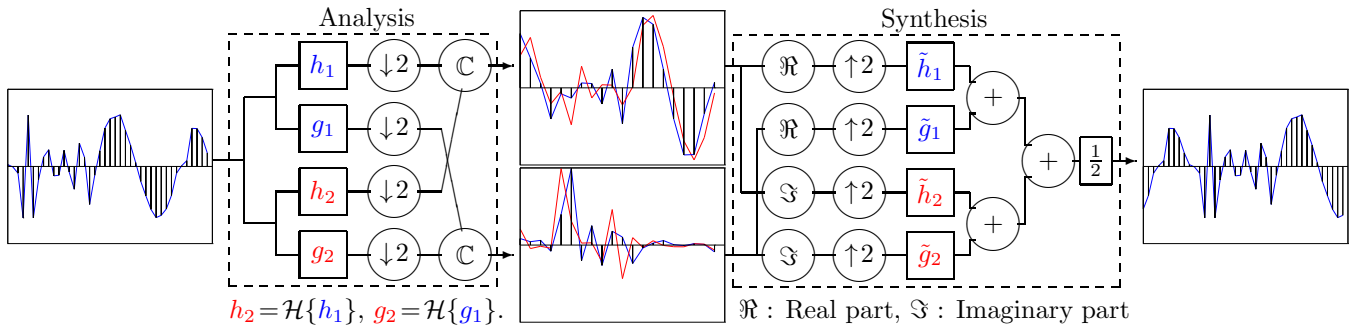


Figure 2: 1D analytic wavelet transform with the Dual-Tree algorithm.

173 performing a CWT as shown Fig. 2 for the 1D case. It is *approximately*  
 174 analytic and achieves *near* shift-invariance with a redundancy of 2:1. These  
 175 two filterbanks lead to four separable 2D filterbanks that can be combined  
 176 to fit the QWT definition. Fig. 1 shows an example of such decomposition.

#### 177 2.4. Interpretation and Use

178 For now, literature is quite poor about QWT and the major difficulty  
 179 with the use of this transform is the interpretation of the phase.

180 In [Bülow, 1999] 2D *quaternionic analytic* Gabor filters are defined and  
 181 used in a Gabor based texture segmentation. Filtered images are 2D ana-  
 182 lytic and form a scale-space analysis of the image; from which are extracted  
 183 *magnitudes* and *local phases* at each point to characterize the texture.

184 A *shift theorem* similar to this of the well known Fourier transform also  
 185 stands for the quaternionic Fourier transform defined in [Bülow, 1999] : a  
 186 shift of the image is equivalent to an offset of the two first terms of phase  
 187  $\varphi$  and  $\theta$ . As a result, in a Gabor decomposition  $\varphi$  and  $\theta$  describe small  
 188 2D spatial shifts of the coded structure - around the quaternionic coefficient  
 189 position. Note that in 1D that shift is equivalent to structural information;

190 but 2D structures may be more complex than lines or edges (*e.g.* corners,  
191 T-junctions) and cannot be described by this kind of shift coding. The third  
192 term  $\psi$  completes the structure analysis and is seen as a texture feature.  
193 Bülou observed that where  $\psi$  is around  $\pm\pi/4$  the coded structure is a line  
194 or an edge oriented along a diagonal.

195 We found three recent references [Chan et al., 2008; Bayro-Corrochano,  
196 2006; Zhou et al., 2007] where  $\varphi$  and  $\theta$  are used in disparity estimation. As  
197 the QWT performs local QFT's; the *shift theorem* approximately stands for  
198 QWT so  $\varphi$  and  $\theta$  code quite simply spatial shifts of structures.

199 In another application of [Chan et al., 2008] ('wedgelet' representation)  
200  $\varphi$  and  $\theta$  are used for wedges position and  $\psi$  is used for their orientation.

201 We propose a new application of this transform : the next section deals  
202 with texture classification. The difference with the work by Bülou is that  
203 while *segmentation* involves detecting where two textures are different, *clas-*  
204 *sification* aims to indicate what kind of texture is observed. In addition, the  
205 tool we use (QWT) is slightly different than Gabor filters in that it is related  
206 to perfect reconstruction filterbanks.

### 207 **3. Texture Classification**

208 Texture classification is the process which - given any textural image  
209 - find the *class* this image most probably belongs to. Texture has still no  
210 universal definition, but may be presented by classical cases like 'tar', 'water',  
211 'sand', as macroscopic examples, or 'town', 'ocean', 'forest', as satellite view  
212 examples; and characterized by a sort of uniformity and periodicity. We call  
213 a kind of texture a *class*; according to an arbitrary classification we humans

214 make instinctively.

215 In this paper, we only discuss wavelet based methods for this applica-  
216 tion in order to compare QWT with DWT. Feature extraction via standard  
217 wavelet representation of images (DWT) has been widely used in texture  
218 analysis [Tuceyran and Jain, 1993; Arivazhagan and Ganesan, 2003; Lasmar  
219 and Berthoumieu, 2010] for the two last decades. Accordingly, the multiscale  
220 analysis provided by the DWT is well adapted to textural images. From each  
221 subband one may calculate a mean, standard deviation, energy, mean power,  
222 or more sophisticated statistical modeling. Those features - well combined -  
223 can form a powerful texture descriptor.

224 The *Dual-Tree Complex Wavelet Transform* (CWT) - a complex exten-  
225 sion of the DWT - is motivating by the near shift-invariance of its magni-  
226 tude and the oriented aspect of its wavelets. It was used in [de Rivaz and  
227 Kingsbury, 1999; Celik and Tjahjadi, 2009, 2011] revealing its efficiency with  
228 respect to DWT in texture analysis. The invariance of magnitude to shifts  
229 makes the extracted feature independent of the precise location of textural  
230 patterns; and so allows a better characterization. We will include CWT  
231 based feature vectors of [Celik and Tjahjadi, 2009, 2011] in our experiments  
232 to compare with literature.

233 We here propose to further texture analysis using QWT because we keep  
234 the advantages due to shift-invariance while adding new information with  
235 the  $\psi$  phase. The QWT can be regarded as the *proper* 2D generalization of  
236 analytic wavelets since the quaternionic analytic signal is the *proper* gener-  
237 alization according to Bülow. We use the Dual-Tree based QWT algorithm  
238 [Chan et al., 2008] and for comparison a DWT with the well known CDF 9/7

239 wavelets. The latter are widely used and offer a good separation of frequency  
240 components; what is well adapted to texture analysis.

241 QWT needs special “Q-Shift” filters designed in [Kingsbury, 2001] to form  
242 Hilbert pairs. Three different filter sets are possible : the 9-tap, 14-tap and  
243 18-tap Q-Shift filters. In wavelet based texture analysis long filters usually  
244 achieve better performance. In this paper we mainly use the 9-tap filters  
245 to ensure fairer comparison with 9/7 classical filters; nevertheless the other  
246 Q-Shift filters will be treated in the experimental part of the paper.

247 A  $L$ -level decomposition provides  $3L$  subbands for analysis and a low-  
248 frequency subband. We do not use the latter; as low frequency structures -  
249 almost constant - are usually not considered to be a feature of texture.

### 250 3.1. Texture Databases

251 In order to provide relevant performance with respect to the huge variety  
252 of textures we can find, we use several known texture databases :

- 253 • Brodatz database [Brodatz, 1966] contains 111 photos called *textures*  
254 by the author. We use those  $[640 \times 640]$  images to create texture *classes*,  
255 by cutting each one into 25  $[128 \times 128]$  sub-images considered to belong  
256 to the same class.
- 257 • Outex databases (<http://www.outex.oulu.fi/>) were specially made  
258 for texture classifiers benchmarking. We use the TC12 database that  
259 contains 24 classes of 380  $[128 \times 128]$  samples. In each TC12 class we  
260 have different images of a same kind of texture at different orientations  
261 and under different lightings.

- 262 • We also use Outex TC14 database, which has 68 classes of 60 samples  
263 with different lightings but only one orientation.

### 264 3.2. Experimental Protocol

265 Recall that our point is the understanding of the QWT. The recognition  
266 scheme must be elementary so we can identify the influence of the choice  
267 of transform/features on the recognition rate. This is why we propose to  
268 use a simple  $k$  Nearest Neighbors classifier ( $k$ -NN) without any automatic  
269 feature selection or normalization that would drown the contribution of the  
270 transform and confuse the interpretation. Note that we use DWT-based and  
271 QWT-based *feature vectors* that will be presented in the next section.

272 Here is the  $k$ -NN algorithm. From each image of a *training base* a fea-  
273 ture vector describing the texture is extracted and labelled by its actual class  
274 number. When a *test image* is given, its feature vector is processed and com-  
275 pared in the *feature space* to the feature vectors of the training base in terms  
276 of Euclidean distance. According to a parameter  $k$ , the  $k$  nearest vectors are  
277 kept to find the most representative class; that is the most represented class  
278 within the  $k$  neighbors.

279 In order to evaluate performance we split our available classes into two  
280 groups :

- 281 • A *test base* :  $N_T$  examples the program does not know;
- 282 • A *training base* :  $N_A$  *labelled* examples the program knows.

283 Then recognition rates obtained by using a certain feature extraction method  
284 will inform about the quality of this method *i.e.* the power of description

285 brought by this feature vector for texture classes. Some classes are better  
286 recognized than others so we can study what kinds of texture make DWT or  
287 QWT more suitable.

### 288 *Cross validation*

289 Since experimental rates will depend on the chosen training base, we pro-  
290 pose to iterate the process 100 times with different selections of the training  
291 base (but fixed  $N_A$ ). We obtain 100 recognition rates for each feature ex-  
292 traction method and each texture class. So our recognition rates will be  
293 displayed as average rates with a certain deviation, following the so-called  
294 cross validation protocol (see Fig. 3 for example). Thanks to cross validation  
295 recognition rates are very stables from an experiment to another (rates vary  
296 less than 1% experimentally).

### 297 *Sample selection*

298 Let us precise how the sample selection is done. We need to separate sam-  
299 ples of each class 100 times differently. If we naïvely pick up  $N_A$  consecutive  
300 samples as they are stored in the database, we introduce a bias due to the  
301 existing correlation between consecutive samples (*e.g.* in TC12 basis, consec-  
302 utive samples have same orientation). So  $N_A$  samples are randomly selected  
303 from each class while the test base is formed by all remaining samples. This  
304 process is repeated at each of the 100 iterations.

305 In the sequel, we first present different feature extraction methods from  
306 DWT/QWT magnitude and QWT phase, as well as complex wavelet features  
307 from [Celik and Tjahjadi, 2009, 2011] for comparison. Then the experimental  
308 classification results related to these descriptors are given and analyzed.

## 309 4. Feature extraction

310 Feature extraction is the automatic processing of several numbers de-  
311 scribing texture characteristics. The output is a so-called *feature vector* that  
312 will be considered in a feature space to compare with other texture samples.  
313 Many wavelet based texture classifications use a global measure of energy  
314 or statistics from the magnitude; which corresponds to characterize partic-  
315 ular bands of the Fourier domain. This type of feature extraction is well  
316 adapted to textures that can be viewed as superimposed signals located in  
317 the Fourier domain. We will study several methods. First we use magni-  
318 tude based features that are analogous for both DWT and QWT. Then we  
319 propose QWT phase based features that will improve texture description;  
320 and a combination of QWT magnitude and phase. Finally the CWT-based  
321 features of [Celik and Tjahjadi, 2009, 2011] - also made of global subband  
322 measures - are described.

### 323 4.1. Magnitude based features

324 After having processed the norm  $M_{ij} = |q_{ij}|$  of wavelet coefficients of a  
325 given image (where  $i$  and  $j$  are discrete coordinate of a pixel); two measures  
326 in each subband are considered.

*Energy :*

$$m = \frac{1}{E} \sum_{i,j} M_{ij}^2$$

327 where  $E$  is the total energy of the image minus the low-frequency energy.  
328 This normalization makes  $m$  the relative amount of energy in a subband.

Standard deviation (*St. dev.*) :

$$m = \sqrt{\frac{1}{N} \sum_{i,j} (M_{ij} - \mu)^2}$$

329 where  $N$  is the number of pixels in the subband and  $\mu$  is the mean.

#### 330 4.2. QWT phase based features

331 We dealt with QWT phase in section 2.4. We will first use some phase  
332 features only and then we combine magnitude and phase information. Now,  
333 how can we use QWT phase to describe textures?

334 First,  $\varphi$  and  $\theta$  are irrelevant because they inform about position of el-  
335 ements whereas we are interested in their structure. We may think of a  
336 matching between the 2D shift coding and some 2D kinds of structure - anal-  
337 ogously to the 1D phase - but this interpretation is not clear. In addition,  
338 our experiments on  $\varphi$  and  $\theta$  gave very bad results (less than 3% recognition).  
339 So we focus on the third term  $\psi$  used by Bülow in a Gabor based texture  
340 segmentation process [Bülow, 1999].

341 In this application we assume that textures are stationary so we do not  
342 want to describe spatially precise texture patterns but rather extract global  
343 measures. However, we want to describe a part of the behavior of the phase  
344 within each subband so a measure such as a *mean* would not be suitable  
345 because it is too global. Experimentally, phase means<sup>1</sup> by subband give very  
346 bad results (less than 1% recognition).

---

<sup>1</sup>The angle is ‘unwrapped’ in the calculus of a mean. But note that  $\psi$  does not show phase wrapping as it lies in  $[-\pi/4; \pi/4]$ .

347 As we aim to do a fair comparison we won't carry out a high level pro-  
348 cess such as spatial measures (extrema search, connexity ...) that would  
349 need to be differently adapted to either DWT or QWT. To make the results  
350 as comparable as possible our application must keep simple and we would  
351 rather extract a single value from a whole subband as a global feature of the  
352 phase spatial behavior. To our knowledge, literature is quite poor about the  
353 measure of phase. The *Global Phase Coherence* [Blanchet et al., 2008] gives a  
354 measure of image sharpness but relies on a too much restricted mathematical  
355 model with respect to the topic of the paper that is a first approach toward  
356 QWT. A *relative phase distribution* measure was used with some complex  
357 wavelets in [Vo et al., 2007] but is specially defined for this type of trans-  
358 form. The quaternionic phase is a totally different concept than the complex  
359 one; so it would be irrelevant to use such a sophisticated measure.

360 It seems that the simple calculus of the standard deviation (st. dev.)  
361 within a subband would be adapted because it describes a part of the behavior  
362 of  $\psi$ . Since  $\psi \in [-\frac{\pi}{4}, \frac{\pi}{4}]$  (see Euler angles) we avoid the usual problems about  
363 circular data ( $\pm\pi$  discontinuity, phase wrapping) so there is no ambiguity to  
364 calculate angle differences and means.

365 To improve robustness the  $\psi$ -deviation can be weighted by the QWT  
366 magnitude. A high magnitude means an important presence of an element  
367 while a low value means 'no element' and also provides a numerically unstable  
368 phase. So the measure should be more representative by not considering the  
369 structure of low magnitude features. The weight function  $W$  is the magnitude  
370 of the QWT coefficients normalized so the sum within the subband is 1; and  
371 is integrated in the standard deviation formula as defined below. Here are

372 the two phase measures we use for feature extraction :

*St. dev. :*

$$m = \sqrt{\frac{1}{N} \sum_{i,j} (\psi_{ij} - \mu)^2}$$

373 where  $\mu = \frac{1}{N} \sum_{i,j} \psi_{ij}$ ,  $N$  is the number of pixels in the subband, and  $(i, j)$

374 spans a subband.

*Weighted st. dev. :*

$$m = \sqrt{\sum_{i,j} W_{ij} (\psi_{ij} - \mu_W)^2}$$

375 where  $\mu_W = \sum_{i,j} W_{ij} \psi_{ij}$  is the weighted mean of the subband.

#### 376 4.3. Combination of QWT magnitude and phase

377 Let us now combine the st. dev. QWT magnitude features with the  
378 weighted st. dev. QWT phase features (Given experimental results that will  
379 be presented in the next section; st. dev. measures are retained for both  
380 magnitude and phase).

381 First we experimentally observed that a simple concatenation of both  
382 vectors gives very good performance - better than DWT. Here is a classical  
383 point in classification : our two features are not of the same kind. One is  
384 an amplitude ( $\in \mathbb{R}^+$ ) and the other is an angle ( $\in [0, \frac{\pi}{2}]$ ). It produces a  
385 lack of coherence in the final feature vector as all that terms are seen the  
386 same way by the Euclidean distance of the  $k$ -NN algorithm. A metric often  
387 solves this heterogeneity problem but the different metrics we tried did not  
388 improve the process. Even considering the optimal metric with respect to our  
389 database; performance is not significantly higher since in practice magnitude

390 and phase features are of the same order of magnitude. So for this paper we  
391 finally consider simple concatenation of QWT magnitude and phase features.

392 To compare with literature we propose to also use CWT. Even though the  
393 concept is totally different from QWT the underlying algorithm is quite sim-  
394 ilar and was used in texture analysis for example in [de Rivaz and Kingsbury,  
395 1999; Celik and Tjahjadi, 2009, 2011].

#### 396 4.4. *Complex wavelets based features*

397 These feature vectors are processed from the 6 subbands of the Dual-  
398 Tree Complex Wavelet Transform (CWT). In most cases, classical features  
399 such as entropy or energy measures as well as statistics are extracted from  
400 the magnitude of each subband. In this experiment we choose to use CWT  
401 magnitude based feature vector from [Celik and Tjahjadi, 2009] that uses  
402 variance and entropy. The very recent work in [Celik and Tjahjadi, 2011]  
403 involves standard deviations and energy measures from both magnitude *and*  
404 phase. Note that in the original paper the vector is further reduced and  
405 weighted based on statistics (PCA) - which we did not reproduce because  
406 our scheme needs to be elementary so we can identify the contribution of  
407 DWT/CWT/QWT (see discussion section 3.2).

408 It is important to stress that the aim of cited papers is to carry out a  
409 good recognition whereas the point of the present paper is the analysis of the  
410 QWT. This is why we do not use the whole recognition process described  
411 in [Celik and Tjahjadi, 2009, 2011] but just the feature extraction bloc. We  
412 refer the reader to original publications for detailed expressions.

413 Now the feature extraction part is done, let us give our experimental  
414 results of texture recognition with every feature vectors described above.

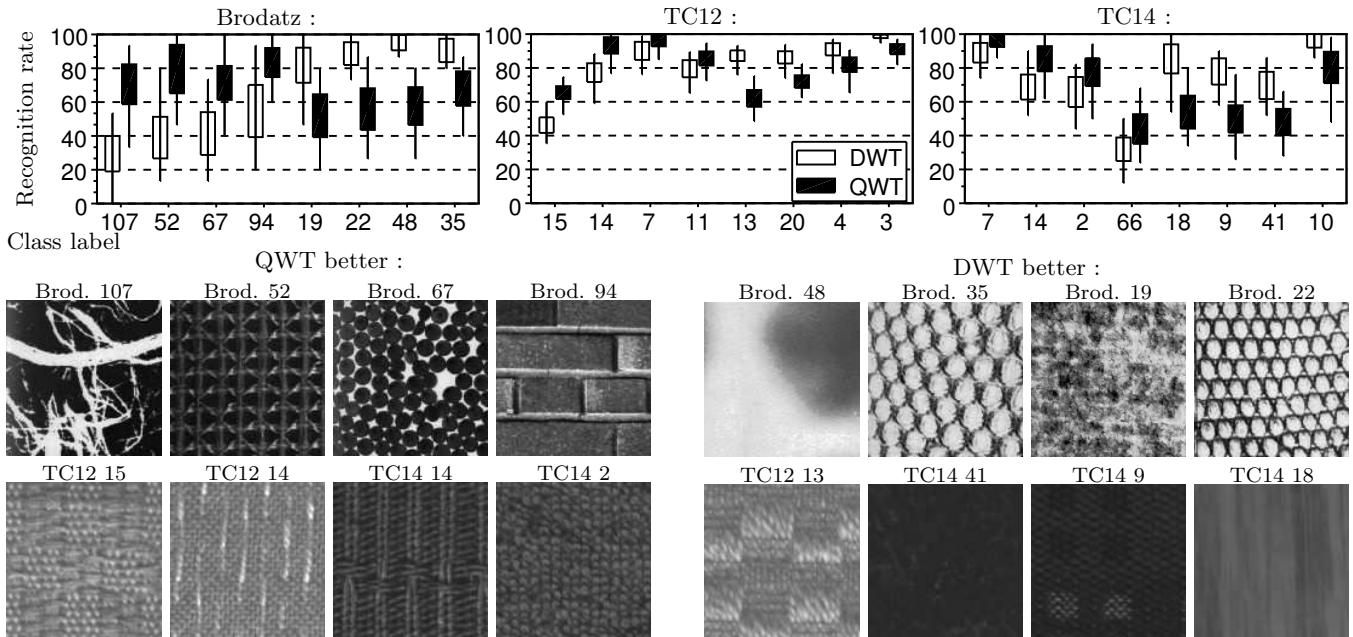


Figure 3: Magnitude based classification performance : cross validation results for some classes of the 3 databases.

415 The next section also brings analysis of interesting types of textures.

## 416 5. Experimental results

417 We obtained many results, depending on  $L$  (depth of wavelet decompo-  
 418 sition), chosen feature extraction, value of  $k$ , size of training base  $N_A$  and  
 419 used database.

420 Experimentally for most feature vectors best results are obtained with  
 421  $L = 3$  and  $k = 3$ . The larger the training base the better the recognition, so  
 422 in this comparative study we consider rather small training bases to put the  
 423 simulation into a rather hard context. The st. dev. measure globally gives  
 424 slightly better performance than energy, so we will only consider the st. dev.

425 feature in the sequel.

426 The choice of Q-Shift filters in Dual-Tree algorithm has almost no influ-  
427 ence on recognition rates (gain is less than 1% recognition). A reason is that  
428 this modification does not affect the first scale (see [Kingsbury, 2001]) so  $\frac{1}{3}$   
429 of features remain the same. So we keep 9-tap filters.

430 For every result presented in the paper, we keep :

- 431 • Depth is  $L=3$  (9 subbands) so feature vectors are of size 9 for DWT/QWT  
432 magnitude and phase features, size 18 for QWT combined magnitude  
433 and phase, size 36 for CWT magnitude from [Celik and Tjahjadi, 2009]  
434 and size 72 for CWT magnitude and phase from [Celik and Tjahjadi,  
435 2011].
- 436 • Number of considered neighbors is  $k = 3$ ;
- 437 • Size of the training base per class is  $N_A = 10$  (resp.  $N_A = 30$  and  
438  $N_A = 10$ ) for Brodatz (resp. TC12 and TC14) database;
- 439 • Magnitude measure is a standard deviation;
- 440 • 9-tap Q-Shift filters are used in the Dual-Tree algorithm.

441 We now present experimental results in terms of recognition rates for DWT/QWT  
442 magnitude based features, QWT phase features, combination of QWT mag-  
443 nitude and phase and CWT based features.

#### 444 *5.1. Magnitude based descriptor : comparing DWT and QWT*

445 Some cross validation results for magnitude based feature extraction are  
446 illustrated Fig. 3. Recognition rates are expressed in terms of mean, standard

447 deviation and extrema of the rates obtained for each class with the various  
448 training bases. Class labels are on the  $x$ -axis and recognition rate on the  
449  $y$ -axis. For each class the vertical line spans all 100 obtained rates between  
450 the minimum and the maximum, the bar is centered on the average rate and  
451 is high two times the standard deviation.

452 Note that globally, both transforms have equivalent performance. We  
453 do not present results for all classes because they are too numerous but we  
454 selected the cases where difference of performance is maximum between DWT  
455 and QWT. These extreme cases could give clues about what type of texture  
456 is better recognized by either the DWT or the QWT.

457 We propose to analyze the results through particular cases to highlight  
458 QWT characteristics. Observing Fig. 3, we see that texture Brod. 67 con-  
459 tains numerous very similar and randomly placed *small black disks*. Shift-  
460 invariance of QWT magnitude is essential to code those structures with vari-  
461 ous positions; whereas each disk is surely quite differently coded in the DWT  
462 because of small space shifts. In this case QWT gives a more robust descrip-  
463 tion of texture - keeping everywhere a coherent representation of the disks -  
464 what explains the superiority of QWT for Brod. 67.

465 Let us call ‘common’ orientations multiples of  $45^\circ$  *i.e.* horizontal, vertical  
466 and diagonal. We can globally see that textures better recognized by QWT  
467 have many structures right aligned with ‘common’ orientations. Those for  
468 which QWT is less efficient rather contain structures oriented *between* them.

469 According to us, this is because QWT phase contains some information  
470 about these intermediate orientations. So by using only magnitude, superior-  
471 ity of QWT is not visible at those cases where many ‘intermediate’ structures

472 are present. But for other cases, this superiority is experimentally confirmed  
473 as the structures are better encoded by QWT magnitude than by DWT -  
474 giving higher recognition rates.

475 To conclude about magnitude based feature extraction, global recognition  
476 performance is quite similar between DWT and QWT. But if we look closer at  
477 particular textures we see that shift-invariance of QWT improves recognition  
478 of textures made of ‘randomly located similar structures’; and that structures  
479 aligned with a multiple of  $45^\circ$  are better represented in QWT magnitude  
480 while other orientations must have their related information in the phase.  
481 And works in [Bülow, 1999] and [Chan et al., 2008] show that QWT phase  
482 can provide a powerful image analysis; making clear that the QWT is not  
483 fully exploited here. Now let us use QWT phase to improve recognition and  
484 outperform DWT.

## 485 *5.2. Contribution of QWT-phase*

486 Quite surprisingly phase based features give performance comparable to  
487 magnitude as shown Fig. 4 - that also contains next results. This is a very  
488 good result. Weighted st. dev. gives much better description than simple  
489 st. dev. what confirms the relevance of less considering phase data of low  
490 magnitude coefficients. In the sequel we only consider weighted st. dev. as  
491 phase measure.

492 All cases occur : for a same texture both magnitude and phase analysis  
493 may be efficient or not - the results are very heterogeneous. It is interesting  
494 to note that many textures are very well analyzed either by QWT magnitude  
495 or by QWT phase - what suggests that the two feature vectors are comple-  
496 mentary. The former gives frequency information like DWT and the latter

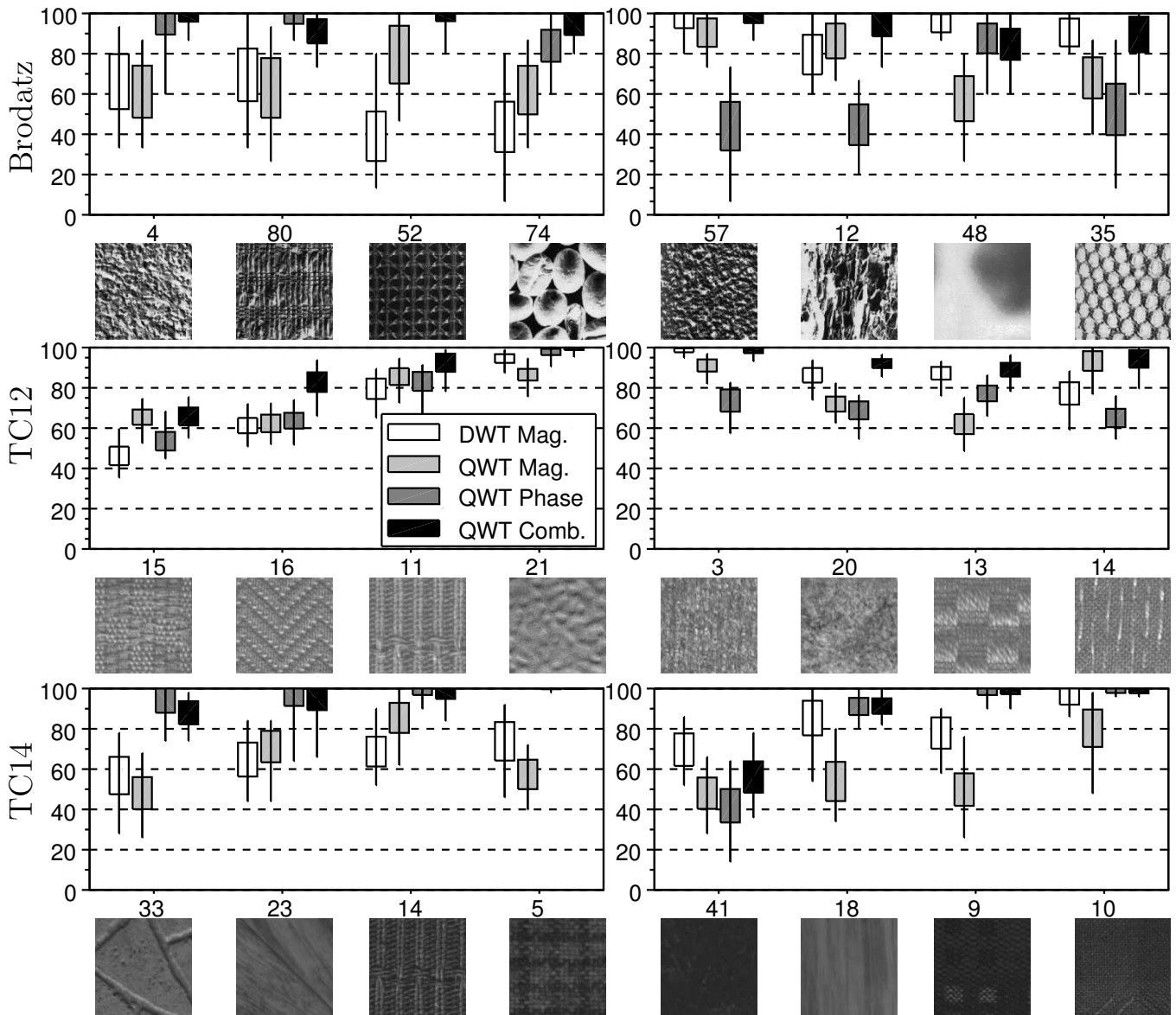


Figure 4: Cross validation results for some classes of the 3 databases. See also Fig. 3. Performance of each class is shown for the measures : DWT magnitude st. dev. (white), QWT magnitude st. dev. (light-gray), QWT phase weighted st. dev. (dark-gray) and QWT combination of magnitude and phase (black).

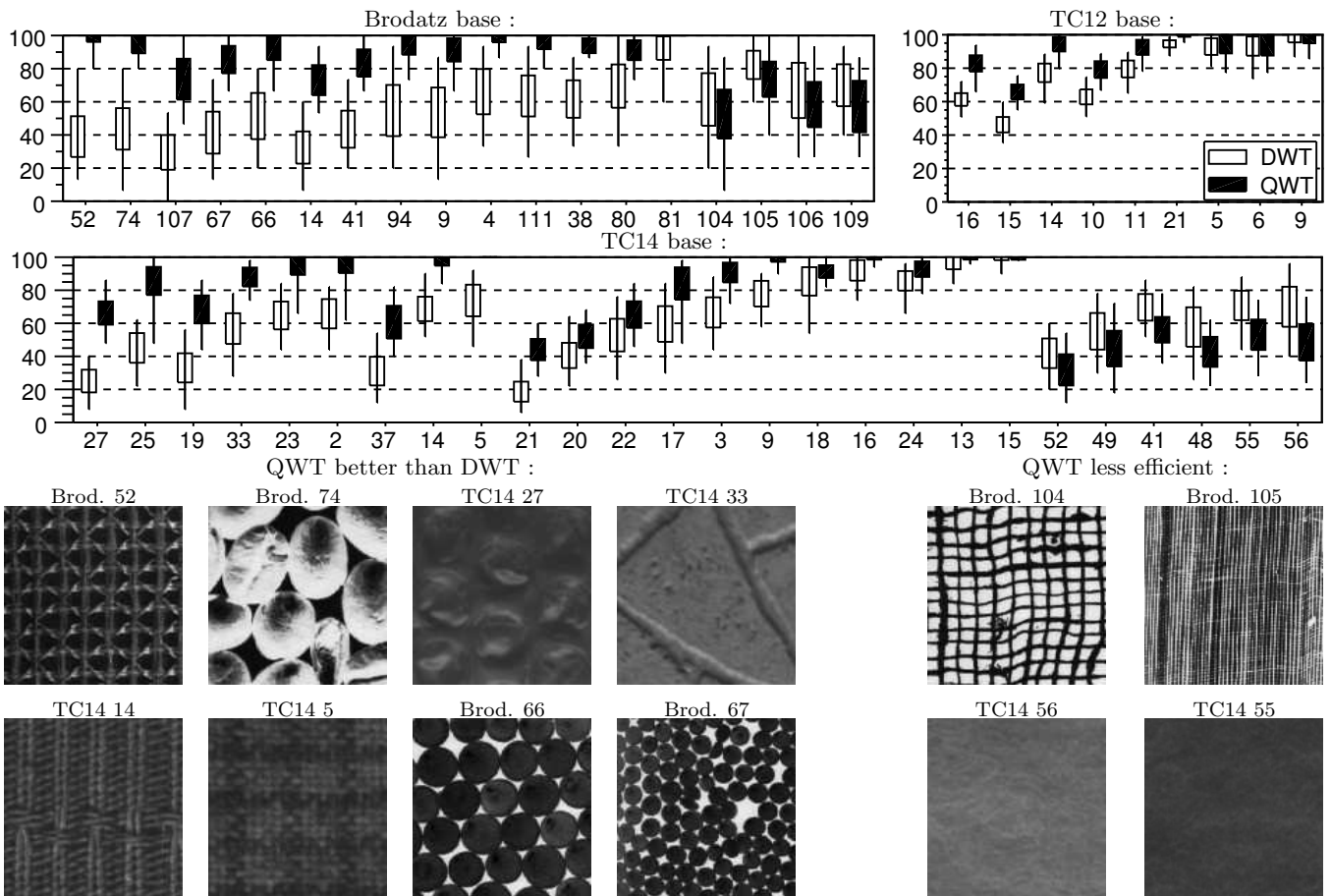


Figure 5: Final classifier performance for the DWT feature vector and the final QWT feature vector using both magnitude and phase.

497 provides additional geometric information.

498 We can hardly identify some kind of textures better recognized by either  
 499 magnitude or phase but the recognition rates really show that magnitude  
 500 and phase are completing one another; so it seems natural to combine both  
 501 feature vectors.

	Brodatz		TC12		TC14	
	Mean	Dev	Mean	Dev	Mean	Dev
DWT Mag.	64%	9	83%	4	56%	8
QWT Mag.	64%	9	82%	4	51%	8
QWT Phase	65%	8	79%	4	58%	6
QWT Comb.	<b>76%</b>	<b>7</b>	<b>91%</b>	<b>4</b>	<b>63%</b>	<b>6</b>
CWT Mag.	65%	8	87%	4	62%	7

Table 1: Final recognition rates.

502 *5.3. Combined QWT magnitude and phase*

503 The final feature vector based on QWT magnitude and phase provides  
504 very good classification performance with an improvement of about 10%  
505 recognition with respect to DWT. We present global recognition rates (mean  
506 rate and standard deviation of obtained rates according to cross validation) in  
507 table 1. As we cannot present every texture class we selected interesting cases  
508 - illustrated Fig. 4 - with recognition rates for respectively DWT magnitude  
509 based feature extraction, QWT magnitude, QWT phase, and final QWT  
510 feature vector. A sample is displayed under each class of the  $x$ -axis. We hope  
511 such an illustration will give some insight about visual texture characteristics  
512 that we could link with QWT properties. Fig. 5 shows more global results  
513 between DWT and QWT to conclude about the general improvement of  
514 classification thanks to the QWT. We have about a dozen ‘bad’ cases but  
515 the overwhelming majority of classes are better recognized by QWT and  
516 figure 5 is very convincing about its superiority.

517 Now we discuss some particular cases to analyze *why* the QWT is better

518 or worse than DWT.

519 A first remark is about texture Brod. 52 that is strikingly better analyzed  
520 by the QWT phase feature vector with 100% recognition. The reason is this  
521 texture contains only horizontal, vertical and - mostly - diagonal structures  
522 that makes  $\psi$  very significant.

523 Most of TC14 classes for which DWT is better are visually similar (see  
524 Fig. 5 TC14 55 and 56), almost uniform and hard to distinguish. These  
525 images have a pure stochastic behavior so the orthogonality of the DWT is  
526 better adapted than the structural analysis brought by QWT - yet this issue  
527 is open.

528 The same remark as in section 5.1 about shift-invariance still holds for  
529 textures Brod. 52, TC14 14 and TC14 5.

530 Note that most textures for which the single QWT magnitude is very  
531 worse than DWT (see Fig. 3) are better represented with the final feature  
532 vector which outperforms the DWT. This result shows that QWT magnitude  
533 and phase are strikingly complementary because both give separately bad  
534 results whereas very efficient when combined. Class TC12 20 (Fig. 4) makes  
535 a good example.

536 Finally, this use of quaternionic representation of textures greatly im-  
537 proves an analogous standard wavelet based texture analysis. We proposed  
538 a wavelet based feature vector that yields an average recognition rate about  
539 10% better than standard wavelets; by using both QWT magnitude - con-  
540 taining similar information than DWT but with shift-invariance - and QWT  
541 phase that provides structural information. Standard DWT does not allow  
542 using such a phase - making it a less coherent representation. With this

543 texture classification we validate the recent QWT from an application point  
544 of view as superior to standard DWT.

545 We will now present experimental results with CWT. Recall that CWT  
546 coefficients are fundamentally different from QWT coefficients in terms of  
547 analysis and interpretation of their geometric meaning. Even if both are  
548 computed by a separable *Dual-Tree* algorithm the combination of the 4 re-  
549 lated filterbank outputs is different. In the QWT case the 4 outputs are  
550 seen like Cartesian components of 3 quaternion valued subbands while for  
551 CWT some *sums* and *differences* of outputs are considered to be real and  
552 imaginary parts of 6 complex subbands - see [Selesnick et al., 2005].

553 This is why analysis provided by CWT has not much to do with QWT;  
554 and we will see in the next section that kinds of texture better recognized by  
555 QWT or CWT - as well as global performance - are not the same.

#### 556 5.4. Results with complex wavelets

557 Results obtained with features from [Celik and Tjahjadi, 2009, 2011] have  
558 to be studied carefully. Recall that we present it to compare with literature  
559 and that we considered only the feature extraction part from cited references.  
560 So result we get are not comparable with the very high performance of orig-  
561 inal papers partly due to a clever choice of classification algorithm together  
562 with proper normalization and feature selection/normalization. In addition  
563 size of training bases may differ.

564 Globally, the first feature descriptor based on CWT magnitude provides  
565 better recognition than DWT but worse than final QWT based features;  
566 which is an expectable result. Second feature vector based on both CWT  
567 magnitude and phase gave very bad recognition (about 5%). We observe that

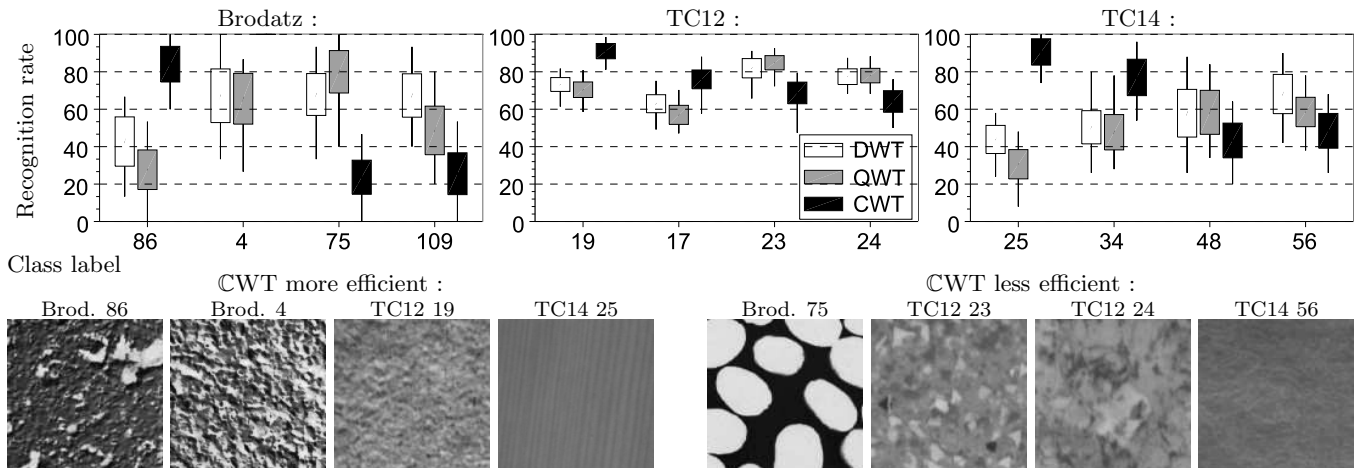


Figure 6: Complex wavelets based classification performance with feature vector described in [Celik and Tjahjadi, 2009]. We selected cases of biggest difference of performance between DWT/QWT and CWT.

568 CWT phase measures are numerically unstable because no special weighting  
 569 is used. In practice many absurd angles - related to the numerous zero  
 570 coefficients - discredit variance end energy features processed on phase data.  
 571 In [Celik and Tjahjadi, 2011] a PCA based feature selection is done before  
 572 classification - what we did not do - so phase based features may be discarded  
 573 by this stage. Thus we will only study magnitude based analysis from [Celik  
 574 and Tjahjadi, 2009].

575 We show Fig. 6 classification results with the first feature vector [Celik  
 576 and Tjahjadi, 2009] in comparison with DWT based st. dev. and QWT based  
 577 final feature vector. Like previous figures, we present only cases of biggest  
 578 difference between different methods.

579 As global rates lie between DWT and QWT (see table 1) we can conclude  
 580 that - by restricting ourselves to simple global features - the oriented behavior

581 of CWT together with shift-invariance of its magnitude can improve a DWT  
582 based analysis but the proposed QWT-phase analysis performs better.

583 An example of the advantage of CWT directionality is texture TC14 25  
584 (Fig. 6). This texture class exhibits straight lines with an orientation around  
585  $75^\circ$ . This is precisely the orientation on which one of the 6 CWT subbands is  
586 aligned. The CWT is well suited in this very particular case so the recognition  
587 performance is much better than DWT/QWT.

588 However directional analysis brought by CWT is globally not as powerful  
589 as the 2D quaternionic phase concept of QWT. The 6 subbands of CWT  
590 offer better frequency selectivity than DWT but it still carry some similar  
591 “energy” information. On the other hand the fundamental relation between  
592 QWT  $\psi$ -phase and geometry provides a new kind of additional information  
593 that complements “energy” data. Finally our results completely confirm that  
594 quaternionic wavelets provide better geometric information than DWT and  
595 CWT for a texture analysis purpose.

## 596 **6. Conclusion**

597 The Quaternionic Wavelet Transform is a recent improvement of standard  
598 wavelets that aims to yield coefficients with a shift-invariant magnitude and  
599 a phase containing geometric information. This transform makes use of a  
600 2D generalization of the analytic signal : a classical powerful tool for signal  
601 analysis. This generalization due to Bülow gives a coherent local analysis of  
602 2D signals and was naturally embedded into a wavelet framework to overcome  
603 common drawbacks of standard wavelets. Redundancy brought by QWT  
604 phase adds complete structural information about local features of images.

605 The QWT is not straightforward to interpret and requires a quite sophisti-  
606 cated theoretical framework. But here we gave an application study crossing  
607 the gap between that framework and the way to use this tool; by showing  
608 its superiority over standard wavelets in a texture analysis context. With a  
609 large texture database our QWT based feature extraction gives globally 10%  
610 better recognition than DWT. This improvement is due to shift-invariance of  
611 QWT magnitude together with the use of QWT phase that contains useful  
612 structural information for texture analysis.

613 A comparison is also made with complex wavelets that have been used  
614 in literature in similar works. Advantage of complex wavelets is good di-  
615 rectionality; which is confirmed in practice by better recognition for some  
616 highly oriented textures. But its complex phase fails to provide such geo-  
617 metric information as this of QWT. As a result QWT outperforms complex  
618 wavelets.

619 Our classification algorithm is a first approach as we focus on studying  
620 QWT so there are many ways of improvements in terms of pattern recog-  
621 nition. In particular, spatial analysis of subbands is not used and the clas-  
622 sification proposed in [Arivazhagan and Ganesan, 2003] for example could  
623 be improved by using a comprehensive use of QWT phase to provide an  
624 excellent classification that could compete with state of the art algorithms.

625 Our future work implies the monogenic wavelet transform - an improve-  
626 ment of the QWT based on another generalization of the analytic signal :  
627 the monogenic signal. This transform is harder to implement but can lead to  
628 a more coherent signal analysis thanks to better properties. Monogenic mag-  
629 nitude is rotation invariant and the phase is easier to interpret than QWT

630 phase.

### 631 **Acknowledgements**

632 This work is supported by the ANR project VERSO - CAIMAN. We also  
633 would like to thank the anonymous reviewer for his/her valuable comments.

### 634 **References**

635 Arivazhagan, S., Ganesan, L., June 2003. Texture classification using wavelet  
636 transform. Elsevier Pat. Rec. Lett. 24 (9-10), 1513–1521.

637 Bayro-Corrochano, E., 2006. The theory and use of the quaternion wavelet  
638 transform. J. Math. Imaging Vis. 24 (1), 19–35.

639 Blanchet, G., Moisan, L., Rougé, B., 2008. Measuring the global phase co-  
640 herence of an image.

641 URL <http://hal.archives-ouvertes.fr/hal-00212337/en/>

642 Brodatz, P., 1966. Textures : A Photographic Album for Artists and Design-  
643 ers. Dover publications, New York.

644 Bülow, T., 1999. Hypercomplex spectral signal representation for the pro-  
645 cessing and analysis of images. Thesis.

646 Celik, T., Tjahjadi, T., 2009. Multiscale texture classification using dual-tree  
647 complex wavelet transform. Pattern Recogn. Lett. 30 (3), 331–339.

648 Celik, T., Tjahjadi, T., 2011. Bayesian texture classification and retrieval  
649 based on multiscale feature vector. Pattern Recognition Letters 32 (2),  
650 159 – 167.

- 651 Chan, W., Choi, H., Baraniuk, R., July 2008. Coherent multiscale image pro-  
652 cessing using dual-tree quaternion wavelets. *IEEE Transactions on Image*  
653 *Processing* 17 (7), 1069–1082.
- 654 de Rivaz, P., Kingsbury, N., 1999. Complex wavelet features for fast texture  
655 image retrieval. pp. I:109–113.
- 656 Hahn, S. L., 1996. Hilbert transforms in signal processing. Artech House,  
657 Boston, London.
- 658 Kingsbury, N., 2001. Complex wavelets for shift invariant analysis and filter-  
659 ing of signals. *Applied and Computational Harmonic Analysis* 10 (3), 234  
660 – 253.
- 661 Lasmar, N.-E., Berthoumieu, Y., 2010. Multivariate statistical modeling for  
662 texture analysis using wavelet transforms. *Acoustics, Speech, and Signal*  
663 *Processing. Proceedings. (ICASSP). IEEE International Conference on.*
- 664 Selesnick, I. W., Baraniuk, R. G., Kingsbury, N. G., 2005. The dual-tree com-  
665 plex wavelet transform. *IEEE Signal Processing Magazine* [123] November.
- 666 Tuceyran, M., Jain, A. K., 1993. Texture analysis. In: *Handbook of pattern*  
667 *recognition and computer vision.* World Scientific Publishing Co., Inc.,  
668 River Edge, NJ, USA, pp. 235–276.
- 669 Vo, A., Oraintara, S., Nguyen, T., 2007. Using phase and magnitude infor-  
670 mation of the complex directional filter bank for texture image retrieval.  
671 pp. IV: 61–64.

672 Zhou, J., Xu, Y., Yang, X., 2007. Quaternion wavelet phase based stereo  
673 matching for uncalibrated images. *Pattern Recogn. Lett.* 28 (12), 1509–  
674 1522.